Intersatellite Calibration of HIRS Upper Tropospheric Water Vapor

Lei Shi and John J. Bates

NOAA National Climatic Data Center, Asheville, North Carolina, USA

Abstract

Intersatellite calibration is carried out for the upper tropospheric water vapor (UTWV) data from clear-sky HIRS channel 12 measurement. As the intersatellite biases are scene brightness temperature dependent, an algorithm is developed to account for the varying biases with respect to brightness temperature. The bias correction data are derived from overlaps of monthly means of each 10-degree latitude belt. For the colder temperature range, data from the simultaneous nadir overpass observations are incorporated. The HIRS measurements from the NOAA series of polar orbiting satellites are calibrated to a baseline satellite. The time series of the intersatellite calibrated HIRS UTWV data from late 1970s to present is constructed and anomaly data are computed. The anomaly time series is used to track tropical waves and variability. The HIRS UTWV anomaly data are particularly useful in monitoring the Madden-Julian oscillation and various equatorial waves.

Introduction

The High-Resolution Infrared Radiation Sounder (HIRS) has been on board the operational National Oceanic and Atmospheric Administration (NOAA) polar orbiting satellite series (N#, where # is the satellite number) for nearly 30 years. Among the twenty channels in the HIRS instrument, channel 12 measures the upper tropospheric water vapor (UTWV). Due to the independence in the calibration based on individual HIRS instrument's channel spectral response function along with other factors, biases exist from satellite to satellite. Fig. 1 shows monthly mean time series of limb-corrected clear-sky HIRS UTWV from each individual satellite of the NOAA polar orbiting satellite series between 30S and 30N. On a monthly basis, the upper tropospheric measurements from different overlapping satellites should reflect similar basic features. However, consistent biases are evident among satellites. For example, the averaged difference between N11 and N12 is -1.2 K. When the HIRS instrument switched from HIRS/2 to HIRS/3, the difference between N14 and N15 is about 8 K. These intersatellite biases have become a common source of uncertainty for long-term studies. The UTWV is a fundamental climate data record and is key to water vapor feedback, so it is important that the intersatellite biases are corrected.

Efforts were made in the past to adjust these HIRS inter-satellite biases. Bates et al. (1996) intercalibrated 13-years (1981-1993) of HIRS time series with an empirical method. In the analysis, the data were binned on 2.5 by 2.5 degree grids for 5-day averaged data. A 13-year mean for each location based on each pentad and each satellite was calculated. The anomaly relative to this mean was then computed for the dataset. The anomalies were compared empirically between two satellites for the same target assuming that the statistical distributions of anomalies were the same. Based on the comparison, the satellites were adjusted to a base satellite (N7) to produce a self-consistent dataset of global observations. Recently, Cao et al. (2005) used simultaneous nadir overpass (SNO) observations to inter-compare radiances measured by HIRS on board N15, N16, and N17. The SNO observations were taken from the same location at the satellite nadir within a few seconds. The method was developed to quantify the observed radiance

differences measured by HIRS on different satellites with little ambiguity. The study also provided extensive discussion on possible causes for HIRS radiance biases.
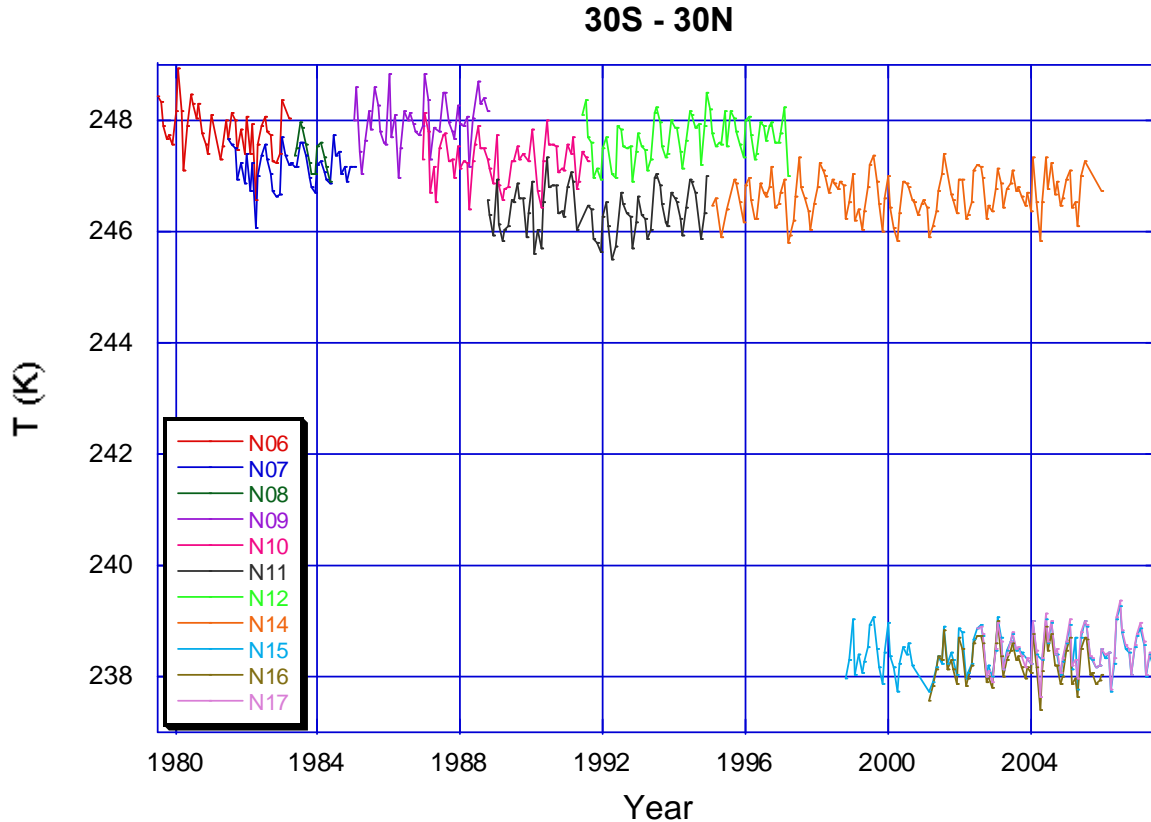
30S - 30N

Fig. 1: Monthly mean time series of HIRS UTWV from each individual satellite, averaged from 30S to 30N latitudes.

Intersatellite Calibration Datasets

The SNO observations provide inter-comparisons of overlapping satellite measurements. However, because the satellites intersect with each other in high latitudes, the data represent only a small portion of the dynamic ranges of global data. In the present study a new approach is developed to derive the clear-sky HIRS intersatellite biases based on matched-up zonal averages from the equator to the poles. On a monthly basis, the global HIRS clear-sky field exhibits distinct zonal features (Wu et al., 1993). We first divide the global data into 10-degree latitude belts from 85S to 85N. Monthly means of these latitude belts are computed. For the overlapping satellites, the differences (biases) of monthly means are obtained along with the monthly mean temperature to account for the temperature dependent features of the intersatellite biases.

The intersatellite biases of UTWV for TIROS-N, N6 to N17, and METOP-2 derived from overlaps of zonal monthly means are shown in Fig. 2. The biases are computed by subtracting the matched-up

brightness temperatures for a later satellite from those for the earlier satellite (for example, the bias between N16 and N17 is $T_b(N16) - T_b(N17)$). For every 2 degree temperature bin of the HIRS observation, the intersatellite biases are extracted and averaged. In the figure, each plot represents the averaged intersatellite bias for the scene temperature centered at the indicated value with the range of -1 and +1 degree K.
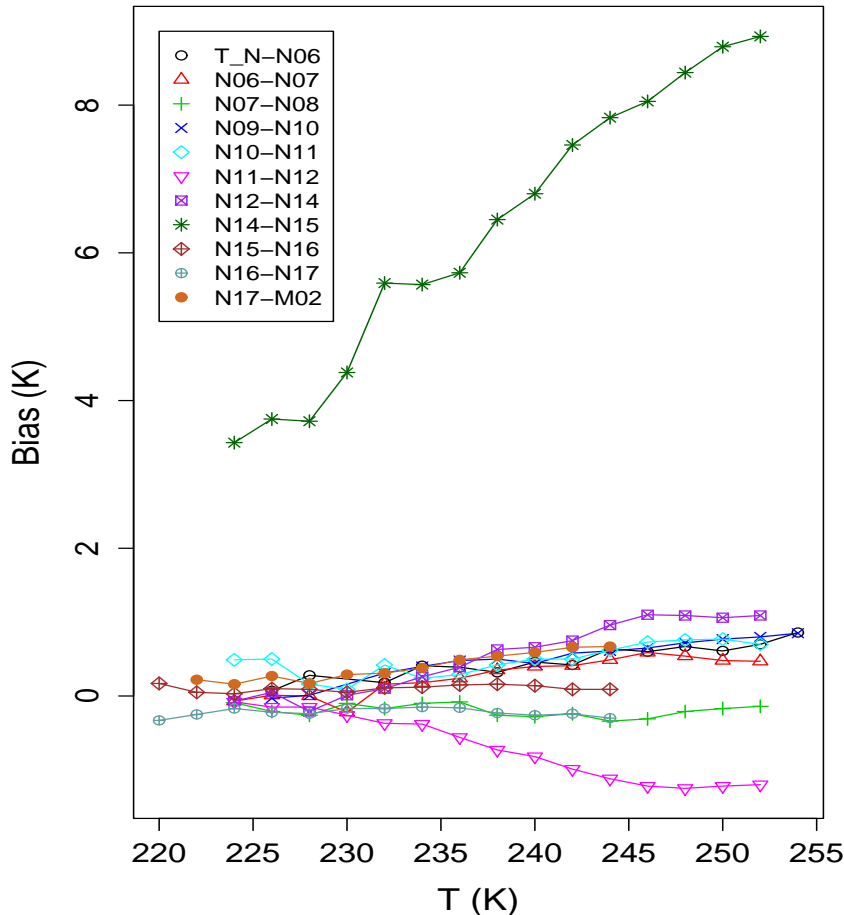

Fig. 2: Sequential intersatellite biases of UTWV for eleven pairs of satellites, as functions of the brightness temperature.

The bias values are very large between N14 and N15. This is caused by the channel frequency change from about 1480 cm^{-1} on N14 and earlier satellites to 1530 cm^{-1} on the KLM series of satellites starting with N15. Due to the frequency change, the sensors on N14 and N15 essentially observed water vapor at different heights, which lead to the large bias of more than 8 K. For other satellite pairs, the biases are within the range of ±0.8 K. Many satellite pairs have bias variations of more than 0.5 K across the scene temperature ranges. Small bias values are found at the low brightness temperature range. Biases generally become larger with increasing brightness temperature.

This bias dataset covers a large range of the scene temperatures. However the monthly means do not cover data at the very low and very high temperatures of pixel observations. For the cooler temperatures,

measurement from SNO observation is used. The SNOs occur when two satellites paths intersect, generally at +70° to +80°, and -70° to -80° latitude zones. Detailed data processing procedure has been provided by Cao et al. (2005). At the high end of the temperature, examinations show that the bias tends to saturate to a constant value (Fig. 2). Therefore for the scene temperatures greater than the ranges in the zonal mean bias dataset, the bias values at the high temperature bound is assigned.

Intersatellite Calibrated UTWV Time Series

The HIRS data are first processed to clear cloudy pixels for the water vapor field. Limb correction is applied with a linear multi-variate regression algorithm using multiple HIRS channels (Jackson et al., 2003). Based on the intersatellite bias dataset, the HIRS channel 12 data from individual satellites are adjusted to N12 as a base satellite. The bias datasets derived from overlaps of zonal monthly means are applied to the scene temperatures except for the coldest scene temperatures, for which biases based on SNO are used. Because there is no overlap between N8 and N9, the intersatellite bias for UTWV between these two satellites are estimated by comparing the time series to the one using methods developed by Bates et al. (1996). An ad hoc bias value of -0.3 K is derived based on the comparison. These bias adjustments are applied to N6 through N17 for each pixel. The pixel data are then mapped to 2.5x2.5 degree grids, and the gridded daily and monthly means are computed.

The intersatellite calibration algorithm is designed to minimize the differences among different satellite measurements. Fig. 3 shows the intersatellite calibrated monthly mean time series of UTWV data from N6 through N17 from 1979 to 2007. A general agreement is found among multiple satellites for the periods that there are overlapping satellites. The large jumps from satellite to satellite displayed in Fig. 1 are removed. The data from the ATOVS satellites (N15 and after) are brought to the TOVS satellite level with similar overall variance between HIRS/2 and HIRS/3. The time series can continually be extended using this method. Comparison of this time series to the one generated based on the algorithm described in Bates et al. (1996) for 1979-1998 also reveals good agreement.

Detailed examination of the intercalibrated time series shows that small differences remain between overlapping satellites. Much of these differences can be explained by the nature of the clear-sky data. The cloudiness condition varies at different observation times of the different satellites. The monthly means for different satellites are thus often the averages of different days in a month, which lead to slight differences in monthly means. To quantify the remaining intersatellite differences that have not been removed by the intercalibration algorithm, the differences of intersatellite-calibrated monthly mean HIRS UTWV between the overlapping satellite pairs are shown in Fig. 4. In the figure each plotted value represents the average of gridded monthly mean differences from 30S to 30N. The difference is calculated by substracting the later satellite value from the earlier satellite value. Fig. 4 displays that the monthly differences of intercalibrated time series are mostly within ±0.2 K, and almost all the monthly differences are within ±0.4 K. The averages of these remaining differences for each pair of the satellites are presented in Table 1. The list shows that the averaged differences are all near zero, and none of the averaged differences is larger than 0.1 K. It is important that the difference clusters of individual pairs of satellites are all closely grouped around 0 K. This ensures that the discontinuities among the uncorrected individual satellite series are minimized in the intercalibrated satellite series.
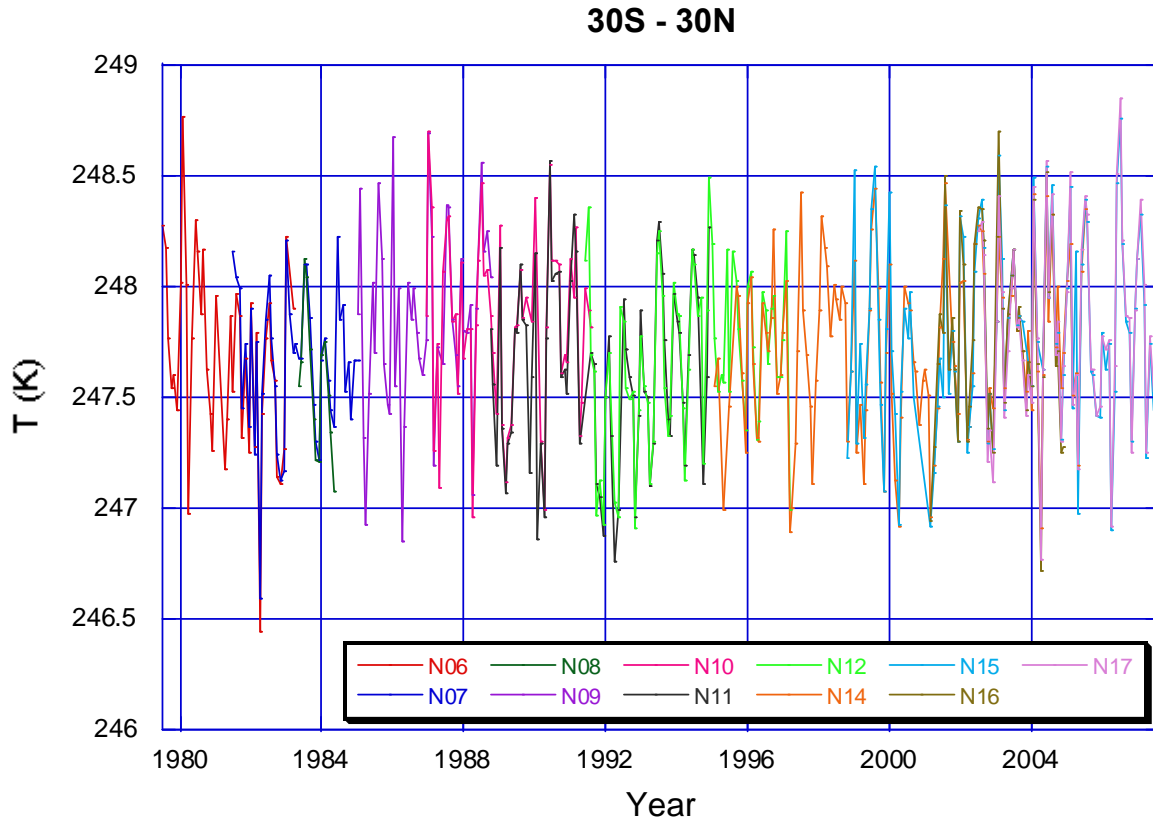
30S - 30N

Fig. 3: Interatellite calibrated monthly mean time series of HIRS UTWV from each individual satellite, averaged from 30S to 30N latitudes.
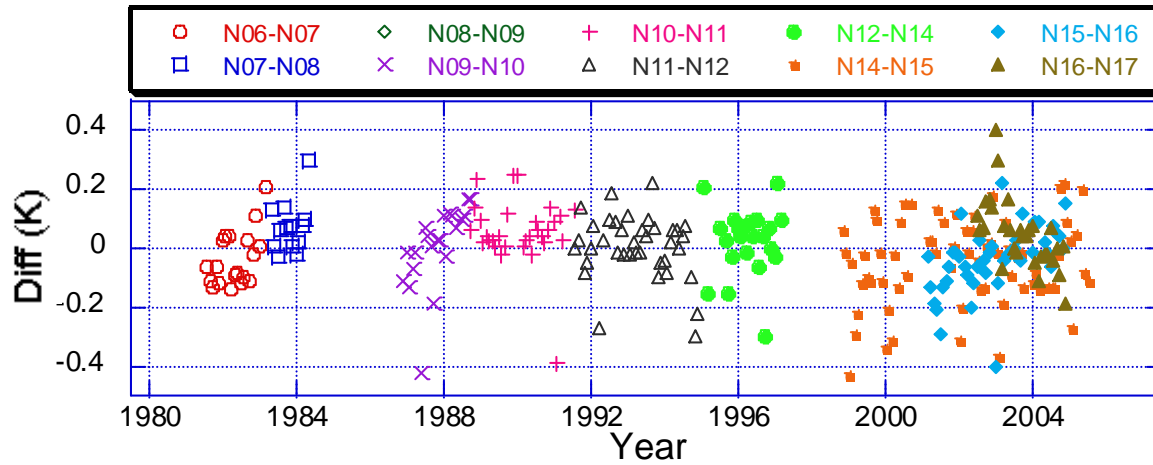

Fig. 4: Differences of intersatellite calibrated HIRS UTWV monthly mean between individual satellites, averaged from 30S to 30N latitudes.

Table 1: Averaged remaining differences (K) of intersatellite calibrated HIRS UTWV monthly mean between individual satellites for 30S to 30N latitudes.

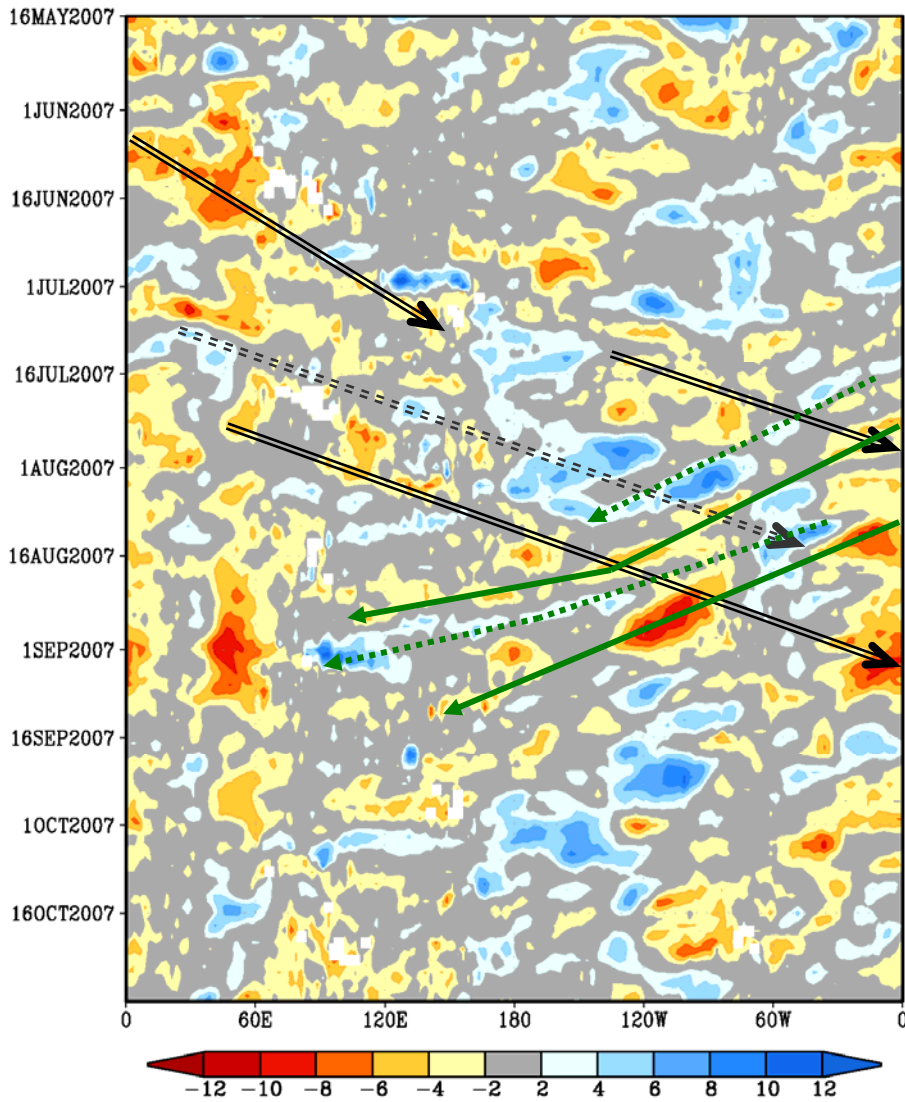| Pairs	N06-N07	N07-N08	N09-N10	N10-N11	N11-N12	N12-N14	N14-N15	N15-N16	N16-N17
Average Difference	-0.065	0.073	0.008	0.059	0.006	0.048	-0.042	-0.035	0.048

Fig. 5: Time-longitude section of clear-sky UTWV anomaly averaged from 7.5S to 7.5N. Shaded colors are the 3-day running mean anomalies calculated by subtracting the daily climatological mean based on the 1979 to 2007 period. The arrows are examples of propagating equatorial tropical waves.

A global UTWV anomaly dataset is developed based on the intersatellite calibrated daily time series. To track and monitor tropical waves, time-longitude section of UTWV data near the equator are examined. The analysis shows that UTWV data have the advantage of around-the-globe coverage of equatorial waves compared to the outgoing longwave radiation data that are currently used by numerical prediction centers. The outgoing longwave radiation analysis typically only captures the tropical waves over the eastern hemisphere. The UTWV provides a continuous observation across both eastern and western hemispheres. Fig. 5 shows a time-longitude section of clear-sky UTWV anomaly averaged from 7.5S to 7.5N for about five months of data. In the figure shaded colors are 3-day running mean anomalies calculated by subtracting the daily climatological mean based on the 1979 to 2007 period. As an example, the black arrows indicate the propagation of several eastward moving Madden-Julian Oscillations, and the green arrows show the westward propagating equatorial Rossby waves which are most significant over the western hemisphere (eastern Pacific Ocean, central America, and Atlantic Ocean). Such a diagram is useful in the continuous monitoring of the movement of Madden-Julian Oscillation and various equatorial waves.

Acknowledgments

References

Bates, J. J., X. Wu, and D. L. Jackson, (1996) Interannual variability of upper-troposphere water vapor band brightness temperatures. J. Climate, **9**, 428-438.

Cao, C., H. Xu, J. Sullivan, l. McMillin, P. Ciren, and Y.-T. Hou, (2005) Intersatellite radiance biases for the High-resolution Infrared Radiation Sounders (HIRS) on board NOAA-15, -16, and -17 from simultaneous nadir observations. J. Atmos. Ocean. Tech., **22**, 2, 381-395.

Jackson, D. L., D. P. Wylie, and J. J. Bates, (2003) The HIRS Pathfinder radiance data set (1979-2001) Proceeding of 12th Conference on Satellite Meteorology and Oceanography, Long Beach, California, February 10-13, 2003.

Wu, X., J. J. Bates, and S. J. S. Khalsa, (1993) A climatology of the water vapor band brightness temperatures from NOAA operational satellites. J. Climate, **6**, 1282-1300.

INTERNATIONAL
ATOVS
WORKING GROUP

Proceedings of the

Sixteenth International

TOVS Study Conference

Angra dos Reis, Brazil

7-13 May 2008

Sharing ideas, plans and
techniques to study
the earth's weather and climate
using space-based observations